Journal of Geospatial Science and Technology 3 (1): 57-73, 2022
DOI: https://doi.org/10.54222/jgst.2022.i4m3txnl
Accepted: July 28, 2022

Comparative Assessment of Nigeriasat-X and Landsat ETM+ Satellite Data in Groundwater Potential Modelling using a part of FCT as Case Study

Olatunji Sunday ABOYEJI and Oluwaseyi Emmanuel OLUWAFEMI

African Regional Institute for Geospatial Information Science and Technology (AFRIGIST), Ile-Ife, Nigeria

Correspondence: *aboyeji@afrigist.org*

Abstract

Groundwater is an important natural resource that supports plants and animal lives. An important factor responsible for its scarcity in developing countries is increasing urbanisation resulting from rapid growth in population and the associated anthropogenic activities. Many studies have used Landsat data for groundwater potential modelling. Information on the usability of NigeriaSat-X data for the same application is limited. The study assessed the utility of NigeriaSat-X and Landsat ETM+ satellite imageries for groundwater potential modelling. The two satellite data, SRTM DEM and other ancillary data were used to generate thematic maps (geomorphological, geological, slope, drainage density, lineament density, NDVI, Soil, and Land cover map). individual themes and their corresponding categories were assigned a knowledge-based ranking from 1 to 5 according to the relative contribution of each of these maps for inferring groundwater potential. GIS-based Analytical Hierarchy Process (AHP) was used to integrate the thematic maps to produce a composite groundwater potential map for NigeriaSat-X and Landsat ETM+. The groundwater potential zones derived were classified ranging from excellent to very poor potential. The modelled groundwater potential zones were validated with field checks and static water level data. Results show that lineament density and geomorphological pattern are the ultimate contributing factors to the occurrence and movement of groundwater in the study area. Areas underlain by migmatite, migmatite gneiss and granitic rocks have moderate groundwater potential, while quartzite and quartz-schist areas exhibit higher potentiality. The study shows that there is no significant difference in the performance of NigeriaSat-X and Landsat ETM+ satellite data for modelling groundwater potential.

Keywords: *NigeriaSat-X, Landsat ETM$^+$, Groundwater, GIS, Remote sensing, Analytical Hierarchy Process (AHP), Comparison*

Évaluation comparative des données satellitaires Nigeriasat-X et Landsat ETM+ dans la modélisation du potentiel des eaux souterraines en utilisant une partie de FCT comme étude de cas

Les eaux souterraines sont une ressource naturelle importante qui soutient la vie des plantes et des animaux. Un facteur important responsable de sa rareté dans les pays en développement est l'urbanisation croissante résultant de la croissance rapide de la population et des activités anthropiques associées. De nombreuses études ont utilisé les données Landsat pour la modélisation du potentiel des eaux souterraines. Les informations sur la facilité d'utilisation des données NigeriaSat-X pour la même application sont limitées. L'étude a évalué l'utilité des images satellitaires NigeriaSat-X et Landsat ETM+ pour la modélisation du potentiel des eaux souterraines. Les données des deux satellites, SRTM DEM et d'autres données auxiliaires ont été utilisées pour générer des cartes thématiques (géomorphologique, géologique, pente, densité de drainage, densité de linéament, NDVI, sol et carte de la couverture terrestre). les thèmes individuels et leurs catégories correspondantes se sont vu attribuer un classement fondé sur les connaissances de 1 à 5 en fonction de la contribution relative de chacune de ces cartes pour déduire le potentiel des eaux souterraines. Le processus de hiérarchie analytique (AHP) basé sur le SIG a été utilisé pour intégrer les cartes thématiques afin de produire une carte composite du potentiel des eaux souterraines pour NigeriaSat-X et Landsat ETM+. Les zones de potentiel des eaux souterraines dérivées ont été classées en classes allant d'excellent à très faible potentiel. Les zones potentielles d'eau souterraine modélisées ont été validées à l'aide de vérifications sur le terrain et de données statiques sur les niveaux d'eau. Les résultats montrent que la densité du linéament et le modèle géomorphologique sont les facteurs contributifs ultimes à la présence et au mouvement des eaux souterraines dans la zone d'étude. Les zones sous-tendues par la migmatite, le gneiss migmatite et les roches granitiques ont un potentiel d'eau souterraine modéré, tandis que les zones de quartzite et de quartz-schiste présentent une potentialité plus élevée. L'étude montre qu'il n'y a pas de différence significative dans la performance des données satellitaires NigeriaSat-X et Landsat ETM+ pour la modélisation du potentiel des eaux souterraines.

Mots-clés : *NigeriaSat-X, Landsat ETM$^+$, Eaux souterraines, SIG, Télédétection, Processus de hiérarchie analytique (AHP), Comparaison*

INTRODUCTION

One of the major concerns in basement complex environments is how to map and monitor the available groundwater resources for various uses (Oikonomidis *et al.* 2015; Rao and Jugran 2003; Singh *et al. 2013*). The complexity and erratic nature of groundwater occurrence in these areas usually make groundwater development in the form of boreholes/wells expensive and arduous (Fashae *et al.* 2014*;* Meijerink 1996). Precise targeting of groundwater resources depends on quality information on the nature of an area's bedrocks and their structural composition, surface morphology and the prevailing climatic conditions (Singh *et al.* 2013; Chatterjee and Dutta, 2022; Ifediegwu, 2022). Aquifers of basement terrains usually occur within the overburden (regolith) and fractured bedrock zones (Fashae *et al.* 2014*;* Wright 1992). They are typically localized (occurring in pockets) and respond to abstraction in a 'discontinuous' fashion, resulting in a low success rate since there are discontinuities or barrier boundaries within the fractures being trapped (Wright 1992). Thus, successful groundwater abstraction requires prior knowledge of the location of good aquifers.

Conventionally, methods such as geological, hydrogeological, geophysical and photogeological techniques are usually deployed to map areas into groundwater potential zones (Anomohanran 2013; Martin and van de Giesen 2005; Okogbue and Omonona 2013; Srivastava and Bhattacharya 2006). While the approaches are suitable for depth-wish characterization of the sub-surface water, they are limited with regard to spatial characterization (Meijerink 1996; Hussein *et al.* 2017). Depth-wish characterization of groundwater is typically based on limited point observations which are costlier and time-consuming to obtain. Even though ground-based methods are indispensable for actual prospecting and drilling of reliable aquifers, the use of geospatial technologies is a means to rapidly narrow down the search for areas where reasonable groundwater can be found (Srivastava and Bhattacharya 2006; Meijerink *et al.* 2007*;* Fashae *et al.* 2014*;*).

Several research works have shown that the integration of remote sensing and GIS-based multi-criteria decision analysis provides an effective means of delineating and mapping areas of groundwater potential. These studies have used satellite data from sensors like Landsat TM, Spot, IRS and others, for groundwater potential zone analyses (Murthy, 2000; Srivastava and Bhattacharya 2006; Krishnamurthy 2008; Dar *et al.* 2011*;* Singh *et al.* 2013*;* Fashae *et al.* 2014*;* Hussein *et al.* 2017; Osinowo and Arowoogun, 2020; Chatterjee and Dutta, 2022; Ifediegwu, 2022). Despite the availability of NigeriaSat-X data and the continuous operation of the platform, little or no studies have used NigeriaSat-X image data for modelling groundwater potential zones. NigeriaSat-X data have been used in studies such as land use/cover assessment, flood disaster monitoring and assessment, crop phenology monitoring, etc., (Agarwal *et al.* 2013*;* Aderoju *et al. 2014;* Ogunmola *et al.* 2014; Saleh *et al.* 2014). The study compared the performance of NigeriaSat-X data for groundwater potential modelling, using GIS-based multi-criteria decision analysis with that of Landsat ETM^+ data.

Location, physical setting and hydrogeology of the study area

The study area lies within longitudes 6° 27′ 00″ E and 7° 23′ 24″ E, and latitudes 8° 15′ 00″ N and 9°12′ 00″ N (Figure 1). Located north of the confluence of the Rivers Niger and Benue, the area is roughly equidistant from points on the national boundary. The area experiences rainy and dry seasons. The rainy season begins in April and ends in October. During this period, daytime temperatures reach between 28°C to 30°C and night-time lows hover around 22 °C to 23 °C (Ifediegwu, 2022). In the dry season, daytime temperatures can soar as high as 40°C and night-time temperatures can dip to 12 °C. The high altitudes and undulating terrain of the territory act as moderating influences on the local climate (Oguntoyinbo *et al. 1978*). The rainfall pattern reflects the

territory's location on the windward side of Jos Plateau to the north. In between the rainy and dry seasons is a brief interlude of harmattan occasioned by the northeast trade wind, with the main feature of dust haze, intensified coldness and dryness (Ojigi, 2005; Ifediegwu, (2022)). The study area falls within the West African Guinean Savanna vegetation belt. There are patches of rainforest in the rugged terrain of the south south-eastern part. These areas form one of the few surviving occurrences of mature forest vegetation in Nigeria.

mica schist, feldspathic quartz schist and migmatites. While some rock outcrops are found in source places, hard rocks are concealed by thin weathered layers in some others. The grey-coloured, massive and homogeneous granites vary from medium to coarse-grained types.

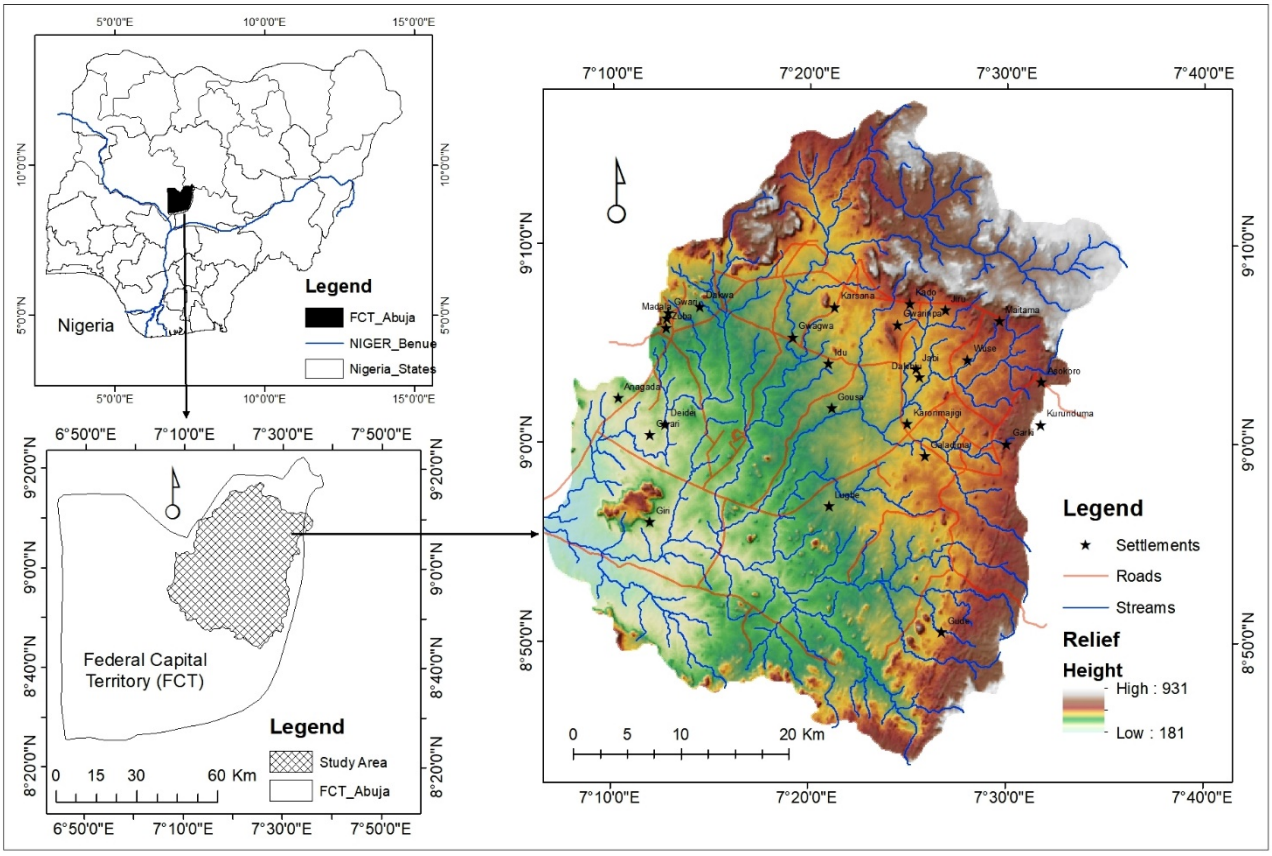

Figure 1: The Study Area

The study area is mostly covered by high-grade metamorphic and igneous rocks of the Precambrian age. The northeast and southwest parts consist of gneiss, migmatites and granites, which generally characterize northern Nigeria. Outcrops of the schist belt, which broadens as one moves southwards, are found along the eastern margin of the area. Like most parts of northern Nigeria, the study area is underlain by basement complex rocks. The rocks around Gwagwalada consist of granite, gneiss, diorites, hornblende schist,

MATERIALS AND METHODS

Description of data used

NigeriaSat eXperimental satellite and Landsat ETM+

The NigeriaSat eXperimental satellite, also known as NigeriaSat-X, is a training model (TM) satellite sensor developed as part of the Know-How Technology Training (KHTT) on the NigeriaSat-2 satellite project. The TM was used as a hands-on project for the Nigerian engineers to master system

requirements specification, project management, system engineering, manufacture, test, assembly/integration and final system testing of a spacecraft (Ikpaya *et al.* 2017). The microsatellite was launched together with the NigeriaSat-2 on 17 August 2011. The satellite was designed for resource management and mapping of territory within Nigerian, specifically for: (1) mapping, monitoring of agricultural activities, and disaster management; (2) serving aa s data continuity solution for NigeriaSat-1; and (3) enhancing national human resources development in space applications and to develop Nigerian capability in space science and technology. The key features of NigeriaSat-X compared to Landsat ETM+ are presented in Table 1. The January 2012 NigeriaSat-X imagery was obtained from the National Space Research and Development Agency (NASRDA), Abuja, while the December 2012 Landsat ETM+ was downloaded from the data archives of the United States Geological Survey (USGS) website.

Development and ranking of factor maps

The first step in groundwater potential zones modelling is the development and ranking of factor maps. Digital image processing and classification of satellite data, conversion of existing analogue maps to digital format, and analysis of field data were employed to generate these layers.

Figure 2 shows the general overview of the methodology adopted. Thematic layers (factor maps) considered for the study consist of geomorphology, geology, slope, land use, lineament, and drainage. These factor maps were generated (separately from NigeriaSat-X and Landsat ETM$^+$ satellite imageries) topographic map, digital elevation model (DEM) and geologic map of the study area.

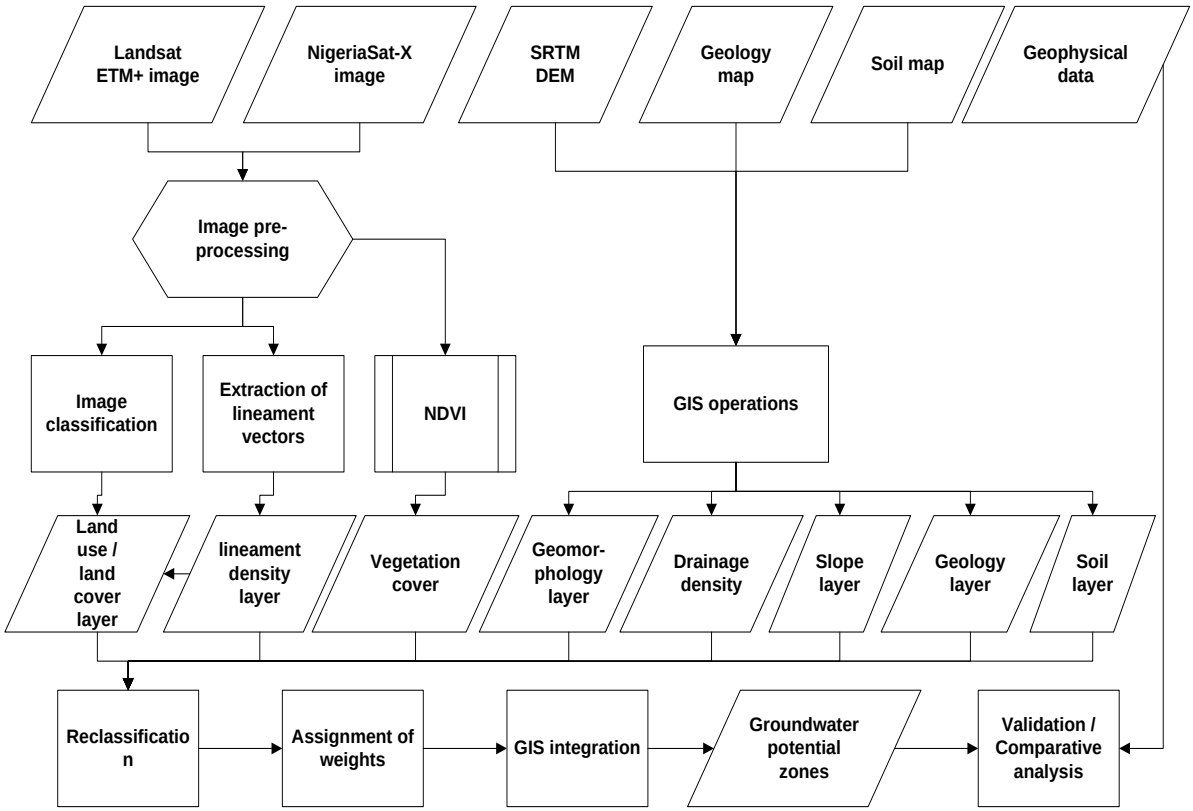

Figure 2: The Workflow Diagram

Table 1: Characteristics of Landsat ETM$^+$ and NigeriaSat-X satellite sensors

Characteristics	Landsat ETM+	NigeriaSat-X
Spatial Resolution	Pan (15m), Multi (28.5m).	Multi (22m)
Radiometric Resolution	8bits	8bits
Temporal Resolution	16 days	3-5 days
Spectral Resolution	Blue - Band 1 (0.45 - 0.515) µm	Green-Band 1(0.52 - 0.62) µm
	Green - Band 2 (0.525 - 0.605) µm	Red - Band 2 (0.63 - 0.69) µm
	Red - Band 3 (0.63 - 0.69) µm	NIR - Band 3(0.76 – 0.90) µm
	NIR - Band 4 (0.75 - 0.90) µm	
	SWIR 1- Band 5 (1.55 - 1.75) µm	
	SWIR 2 - Band 7 (2.09 - 2.35) µm	
	TIR - Band 6 (10.4 - 12.5) µm	
Swath Width	185 km	600 km
Altitude	705 km Sun-synchronous	700 km Sun-synchronous
Launch Date	4/15/1999	8/17/2011

Structural lineaments

The occurrence of groundwater in hard rock terrains, such as the study area, is often related to areas where fractures and faults had occurred (*Fashae et al.* 2014*;* Prasad *et al.* 2008). Lineament-length density was thus considered an important indicator of the degree of rock fracturing which significantly affect the occurrence and movement of groundwater in the study area. The lineament-length vectors within the study area were generated from NigeriaSat-X and Landsat ETM+ satellite images An Edge detection algorithm was used to derive gradient images. Thresholding was used on the gradient images to create binary edge images from where the lineaments were automatically extracted in PCI Geomatica 9.1 software environment. The lineament density map was generated from lineament-length vectors derived from the two images using the focal statistics module of ArcGIS 10.4 software. The final lineament factor layer was reclassified into five density classes, from very low to very high (Figure 3).

The study area is crisscrossed with structural lineaments resulting from several tectonic activities that have occurred in the past. They tend to align prominently in N–S, NE–SW and NW–SE directions. In almost all of the study area, lineament lengths vary from less than 0.021km to 6.714km for NigeriaSat-X and 0.030km to 5.007km for Landsat ETM+ (Figure 3). The distribution of lineament density suggests geologic control with areas underlain by migmatite gneiss and granites showing lower lineament lengths and lineament densities compared to areas underlain by meta-sediments (composed of schist, quartzite and meta-conglomerate), which have higher lineaments and lineament densities. Thus, areas with higher lineament density are regarded as good for groundwater development (Hussein *et al.* 2017*;* Nampak *et al.* 2014).

Normalized Difference Vegetation (NDVI) layer

Normalized Difference Vegetation Index (NDVI) values are a measure of the presence and condition of green vegetation. The transformation is important for detecting groundwater-bearing fractures and faults, due to vegetation response (Meijerink *et al.* 2007). The procedure involves a non-linear transformation of red (R) and near-infrared (NIR) bands of satellite images (Equation 1). The value usually ranges from -1 to 1.

$$(\mathrm{NIR} - \mathrm{Red})/(\mathrm{NNIR} + \mathrm{Red}) \quad \ldots\ldots\ldots$$
Equation 1

For this work, the index was used to estimate the abundance of vegetation patches that have responded to the preponderance of groundwater in the geographic space of the study area. The NDVI maps were generated for NigeriaSat-X and Landsat ETM+ imageries (Figure 3).

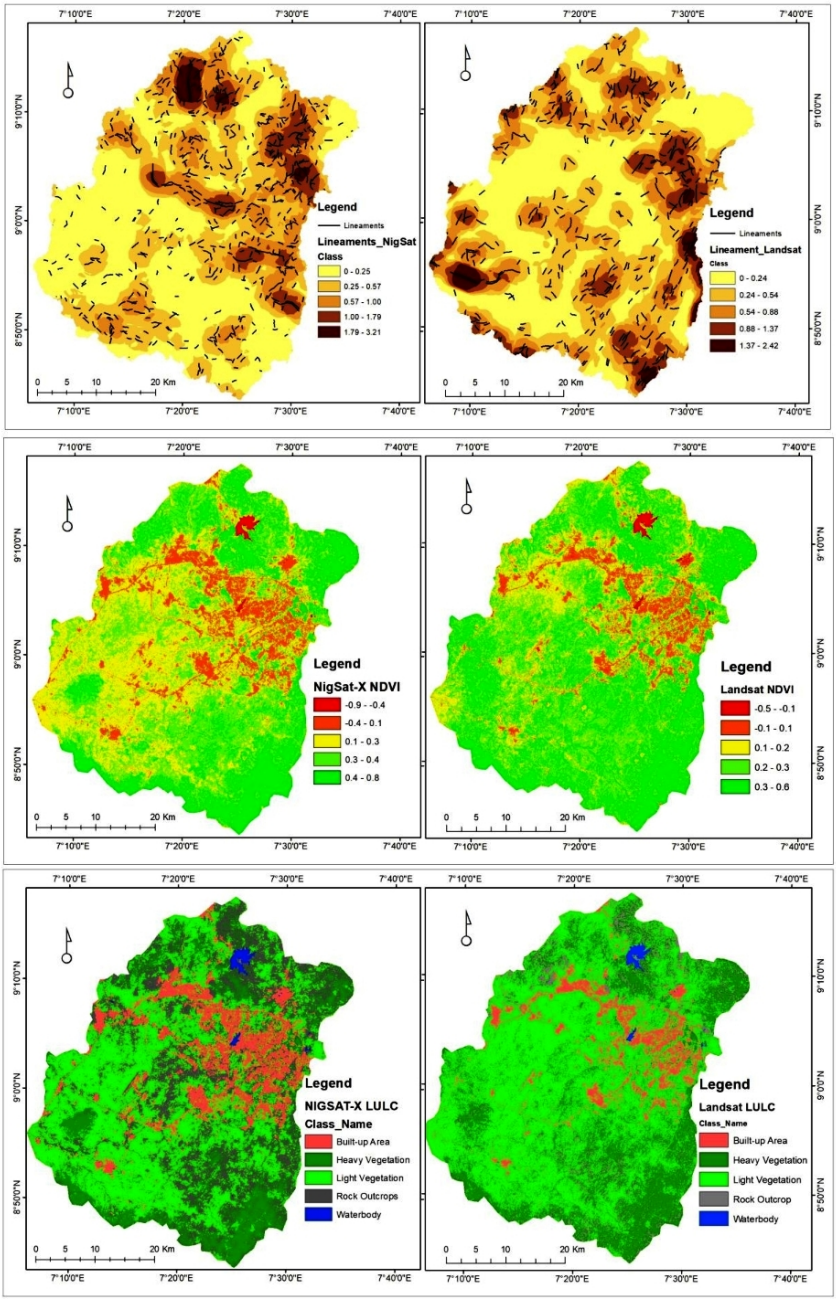

Figure 3: (a) Lineament vectors and density obtained from NigeriaSat-X (left) and Landsat ETM+ (right); (b) NDVI derived with NigeriaSat-X (Left) and Landsat ETM+ (Right); and (c) land cover gotten from NigeriaSat-X (left) and Landsat ETM+ (right)

Land use/land cover layer

The occurrence and recharge of groundwater are governed by the nature and spatial pattern of land use/cover (LULC) of a terrain. LULC consist of the preponderance of soil type, the nature of human activities, and vegetation cover. The land LULC factor map for the study area was generated using NigeriaSat-X and Landsat ETM+ satellites data. Bayesian Maximum Likelihood Classifier (MLC) was used to classify the two images. The land uses and covers were weighted and classified for groundwater potentiality in the order of Built-up area < Waterbody < Rock Outcrop< Light Vegetation< Heavy Vegetation. The main land uses/covers in the study area are heavy vegetation (natural forests and plantations), light vegetation (farmland and grass), water bodies (stream and lakes), built-up areas and rock outcrops (Figure 3).

Lithology

The bedrock of the study area is typified by Basement Complex rocks, a common characteristic of the Precambrian unit of the West African Craton. The bedrock consists of igneous and metamorphic rock types (granites, schist, quartzites, migmatite gneisses, and metasediments). Schist and meta-sediment are in the low-lying areas, while elevated topographic ridges and scattered inselbergs are mainly of quartzite and granite gneiss origin. The lithological layer of the study area was derived from the existing analogue geologic map. The map was scanned and geo-referenced in ArcGIS 10.2.1 software environment. Different rock types were digitised on-screen into separate polygons. As unfractured Basement Complex rock formations normally have little influence on groundwater occurrence apart from situations in which secondary porosity through the development of weathered overburden and fractured bedrock units occurs. Hence, based on the presence and nature of the weathered units and fracture systems, the rocks were reclassified and appropriate weights are assigned (Figure 4).

Soil layer

The soil characteristics of a terrain influence the amount of water infiltrating the bedrock and the rate of groundwater recharge. Infiltration rate is governed by soils' grain size and is closely related to the hydraulic characteristics of the soils (Fashae *et al.* 2014). Fine-grained soils usually limit the rate of infiltration as opposed to the permeable coarse-grained soil materials in which water can easily infiltrate. Porous and permeable soils such as sandy loam types are good indicators of groundwater potential. Impermeable soils like clay, though very porous, but doesn't allow much percolation. For this study, the existing soil map of the entire country was used as the base to derive the soil layer for the study. The main soil types are Arenosols, lixisols and leptosols. Based on the soils' infiltration rate, they were reclassified as sandy, sandy loamy and loam clay soils (Figure 4). Sandy soils were assigned the highest weight, being coarsest and most permeable, and loamy clay was assigned the lowest priority because it has the least rate of infiltration in the group.

Slope

Slopes in general affect the residence time of surface water on the terrain before it infiltrates or flow downslopes. High slopes produce high runoff with short residence time for infiltration and recharge. Greater velocity of rainwater and low groundwater recharge occur on steep slopes (Oikonomidis *et al.* 2015; Chatterjee and Dutta, 2022), while groundwater potentiality increases with lower slopes due to greater infiltration. The slope map (Figure 4) indicates a range of less than 2.8° (i.e., nearly flat surfaces to very gentle slopes) to 55.7° (very steep). The wide range and distribution of the slopes show that the study area is varied in run-off and recharge, implying varied groundwater potential characteristics. With respect to water infiltration and groundwater recharge, the flatter areas were rated higher than slopes greater than 20.6° in terms of groundwater potentiality.

The slope layer was calculated on the pixel basis using the SRTM digital elevation model (DEM) using the spatial analyst tool of ArcGIS 10.3 Software. Classes having low values were assigned higher ranks, and higher slope classes were categorized lower ranks.

Drainage and drainage density layer

Drainage density of a terrain, expressed as the total length of all streams/rivers in a catchment divided by the catchment's total area, reflects the frequency of drainage line through which water leaves the catchment as runoff. It is governed by its geomorphology, geology, and the prevailing climatic environment, among other factors. Other things being equal, impermeable, rugged, and high relief areas usually experience more surface runoff than flat and gently sloped terrains. The denser the drainage networks the less the rate of recharge, and vice versa. Hence, the higher the drainage density, the greater the propensity of surface runoff and the lower the probability of groundwater recharge or potential groundwater zone, and, vice versa (Agarwal *et al.* 2013*;* Fashae *et al.* 2014*;* Singh *et al.* 2013, Bhunia, 2020).

The drainage network within the study area was generated using on-screen digitizing of geo-referenced 1:50,000 topographic maps. The vectors generated were burnt into SRTM DEM in ArcSWAT extension of ArcGIS 10.3 software environment to derive the drainage networks. The drainage density layer was generated by clipping the drainage networks into sub-basins of the study area. For each basin, drainage density (km/km^2) was calculated as

$$Dd = \frac{\sum_{i=1}^{i=n} N_1}{A} \qquad \text{.... Equation 2}$$

where $\sum_{i=1}^{i=n} N_1$ is total drainage lines N1 for a basin and A is the basin's land area in km2.

With respect to groundwater potentiality, the map was reclassified and areas of low drainage density ranked higher than areas of high drainage density. The drainage density of the study area ranges from 0.28km per km^2 in the northern part, to 1.63km per km^2 in the south (Figure 4).

Geomorphology layer

The character of an area's landform determines the occurrence and distribution of groundwater. It helps in understanding the processes, materials/lithology, structures, and geological controls relating to the occurrence of groundwater. For this study, with respect to elevations and the shape of landforms, four types of geomorphological units were identified and delineated. These are plains, lowlands, hills/ridges and inselbergs (Figure 4). Plains are gently rolling relatively flat terrains that do not change much in elevation within a common area, while lowlands are defined as areas having nearly level ground and low elevation with respect to the mean sea level. Plains and lowlands consist of deeply weathered rock materials and are the most favourable zones for groundwater accumulation and percolation. The quantity of groundwater storage is a function of the thickness of weathered material and land cover. The ridges and inselbergs represent chains of high grounds. They are characterized by moderate to steep slopes and high drainage densities and are zones of poor groundwater accumulation zones as they act as runoff zones (*Singh et al. 2013*). These geomorphic units were determined using DEM and satellite image data and were ranked based on their potential contribution to groundwater recharge. They were weighted and classified for groundwater potentiality in the order of inselberg < ridge < plain < lowland.

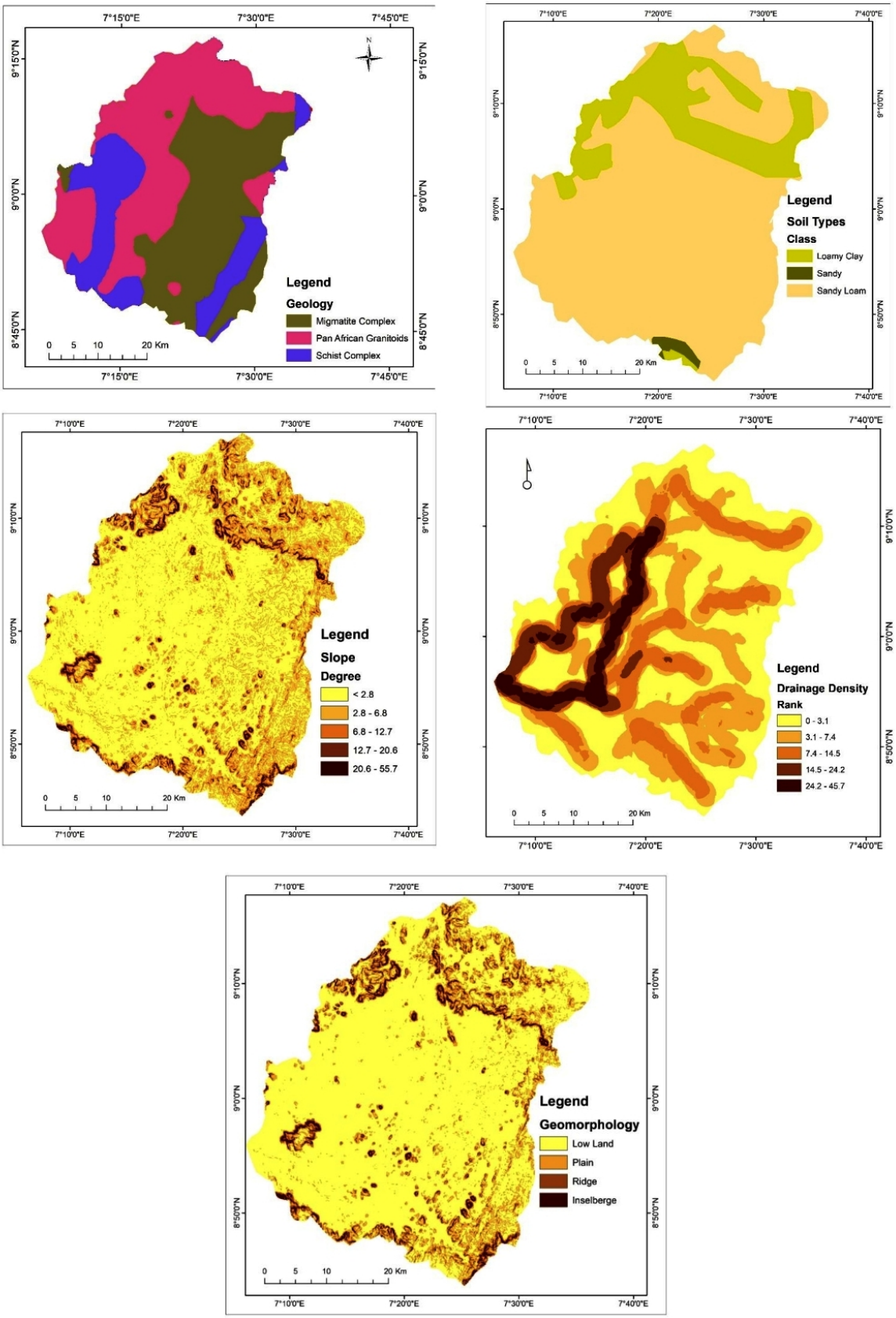

Figure 4: Reclassified (a) geology, (b) soil, (c) slope, (d) drainage density and (e) geomorphology of the study area

Table 2: Saaty's scale for assignment of weights and its interpretation (Saaty 1980; Saaty 1986)

Less important				Equally important	More important			
Extremely	Very strongly	Strongly	Moderately	Equally	Moderately	Strongly	Very strongly	Extremely
1/9	1/7	1/5	1/3	1	3	5	7	9

Weights 2, 4, 6 and 8 are intermediate values that denote compromise.

A pairwise comparison matrix was derived using Saaty's nine-point importance scale based on the thematic layers used for delineating groundwater potentiality (Table 3). The uncertainty in judgements was calculated using the principal eigenvalue and Consistency Index (CI) (Saaty, 2004).

The Consistency Ratio (CR), a measure of the consistency of the pairwise comparison matrix, was calculated by Equation 4.

$$CR = \frac{CI}{RI} \quad \ldots\ldots Equation\ 4$$

where RI is the Ratio Index. The value of RI for different n values is given in Table 4.

Table 3: Pairwise comparison matrices of factors of groundwater potential

Parameters	**NDVI**	**Soil**	**Slope**	**Geology**	**Land Cover**	**Geomorphology**	**Drainage Density**	**Lineament Density**
NDVI	1							
Soil	2	1						
Slope	3	2	1					
Geology	4	3	2	1				
Land Cover	5	4	3	2	1			
Geomorphology	6	5	4	3	2	1		
Drainage Density	7	6	5	4	3	2	1	
Lineament Density	9	8	7	6	5	4	3	1

Consistency Ratio = 0.03

The Consistency Index was derived using equation (Equation 3).

$$CI = \frac{\lambda_{max} - n}{n-1} \ldots\ldots\ldots Equation\ 3$$

where λ_{max} is the largest eigenvalue of the pairwise comparison matrix and *n* is the number of criteria or factors.

Saaty (2004) suggests that the value of CR should be less than 0.1, otherwise the inconsistency of the pairwise comparison matrix is unacceptable, and the corresponding weights need to be re-evaluated (Malczewski and Rinner 2015). The CR of the pairwise comparison matrix obtained is 0.03, which is less than the threshold value. The weights assigned to each factor map are shown in Table 5.

Table 5: Rank and weight of factor layers used for groundwater potential modelling

Criteria	Classes	Rank	Weight
NDVI	-0.93 – -0.48	1	0.1111
	-0.49 - 0.12	2	
	0.13 – 0.26	3	
	0.27 – 0.38	4	
	0.39 – 0.79	5	
Soil	Sandy soil	5	0.0527
	Sandy Loam	4	
	Loamy Clay	2	
Slope	0 - 2.8 degree	5	0.1750
	2.8 - 6.8 degree	4	
	6.8 -12.6 degree	3	
	12.6 -20.6 degree	2	
	20.6 – 55.7 degree	1	
Geology	Granite Gneiss	5	0.0745
	Migmatite	4	
	Migmatite Gneiss	4	
	Biotite	1	
	Quartzite	3	
	Undifferentiated Schist	2	
	Muscovite	2	
	Porphyroblastic gneiss	1	
Land cover	Heavy Vegetation	5	0.0787
	Light Vegetation	4	
	Rock Outcrop	3	
	Waterbody	2	
	Built up	1	
Geomorphology	Lowlands	5	0.2145
	Plains	4	
	Ridges	2	
	Inselbergs	1	
Drainage density	24.2 - 45.7 km	1	0.0649
	14.5 - 24.2 km	2	
	7.4 - 14.5 km	3	
	3.1 - 7.4 km	4	
	0 - 3.1 km	5	
Lineament Density	< 0.11 km	1	0.2285
	0.12 - 0.30 km	2	
	0.31 - 0.53 km	3	
	0.54 - 0.81 km	4	
	> 0.82 km	5	

The final groundwater potential zone (GWPZ) ap was derived through the weighted overlay technique (Equation 5).

$$GWPZ = (NDVI \times 0.1111) + (Soil \times 0.0527) + (Slope \times 0.1750) + (Geology \times 0.0745) + (Land\ cover\ \times 0.0787) + (Geomorphology \times 0.2145) + (Drainage\ density \times 0.0649) + (Lineament\ Density \times 0.2285) V(A_i) = \sum_{k=1}^{n} w_k v(a_{ik}) \quad \ldots \text{Equation 5}$$

Based on the assignment and weighting of the individual features of the thematic layers, a potential groundwater index maps were produced for NigeriaSat-X and Landsat ETM+ satellite data. The groundwater potential maps were grouped into five classes of very high, high, moderate, low and very low classes using quantile classification method (Nampak *et al. 2014*).

Validation of groundwater potential zones model with borehole yield data

The results were validated with borehole yield data. The aquifer of the different locations was characterised with Vertical Electrical Resistivity (VES) survey data collected at 35 different locations using Schlumberger Electrical Resistivity technique spread over the study area (Srivastava and Bhattacharya 2006). The apparent resistivity values obtained were plotted against the inter-electrode spacing AB/2 on a bi-log graph paper, the data points were then joined manually with smooth curve and interpreted using partial curve matching method. The resistivity and thickness obtained were appropriately refined using a WinResist software algorithm.

RESULTS AND DISCUSSION

Groundwater potential zonation

Figure 5 shows the groundwater potential zones derived from NigeriaSat-X and Landsat ETM+ satellite data. The groundwater potential map derived using NigeriaSat-X as the main data input shows that classes Very Low, Low, Moderate, High and Very High are 20.2%, 20.0%, 20.0%, 19.8% and 19.9% of the study area, respectively. Landsat ETM+ on the other hand shows Very Low, Low, Moderate, High, and Very High to be 20.2%, 19.8%, 20.7%, 20.7% and 19.3%, respectively (Table 6).

The groundwater potential maps of the two-satellite data show that lineament density and geomorphological pattern are the ultimate contributing factors to the occurrence and movement of groundwater in the study area. Geologically, consisting of migmatite and migmatite gneiss bedrock characterized by relatively low lineament density have moderate groundwater potential. On the other hand, areas underlain by quartzite and quartz-schist, being more deeply weathered and fractured exhibit higher groundwater potential. Zone with granitic rocks portrays moderate groundwater potentiality. The findings corroborate Murthy and Mamo (2009) and Fashae *et al. (*2014*)* who found the groundwater potential zones of crystalline basement terrain to be poor in the migmatite and migmatite gneiss formations, and very good to moderately good potential in the areas underlain by migmatite and quartzite rock units. The generally high percentage of low to very low groundwater potentiality of both NigeriaSat-X and Landsat ETM+ is a confirmation of the generally limited aquiferous capability of Basement Complex terrain (Fashae *et al.* 2014*;* Talabi and Tijani 2011).

to high groundwater potential in the two

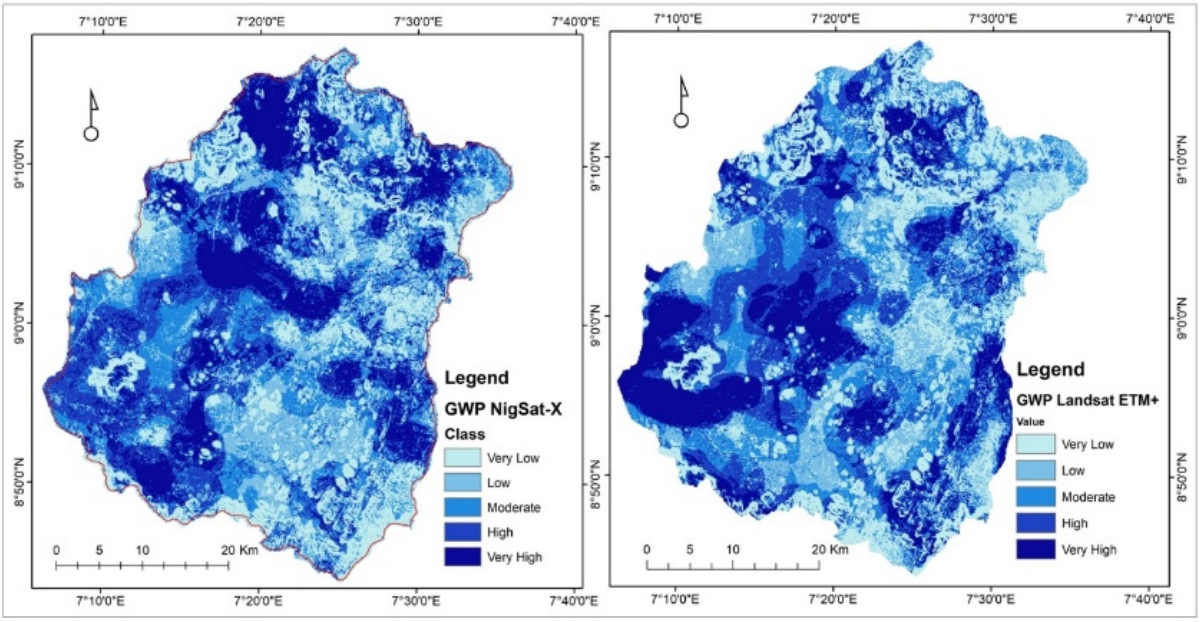

Figure 5: Groundwater Potential Zones derived using Landsat ETM+ and NigeriaSat-X Satellite data

Validation of groundwater potential zones

Validation of the groundwater potential zones was checked against Static Water Level (SWL) data of 35 borehole locations within the study area. Water table depths interpreted from Vertical Electrical Sounding (VES) curves derived for each borehole were taken to represent the actual groundwater levels. The curve types consist of A, H, HA, KH, and HKH (Table 6). The KH and HKH curve types indicate fracturing and are favourable zones for groundwater abstraction. The H types curve is commonly water saturated and often characterized by low permeability, high porosity and low yield (Oladapo *et al.* 2004).

In general, the static water level ranges from 8.5 – 23.5 metres, which reflects the typical varied nature of the water-bearing zones of basement complex formations such as the study area. Comparison of the static water level data with the groundwater potential maps generated shows that 85% of the locations with > 15m static water level fall within areas of low to very low groundwater potential reported by both NigeriaSat-X and Landsat ETM+ models. Also, 75% of the borehole locations with static water levels below 15m have moderate

This suggests that the groundwater potential models substantially approximate the true groundwater depths/potentials of the study area. Thus, GIS-based multi-criteria analysis techniques can be used rapidly scan terrains for location of good aquifers in a cost-effective manner, compared to the traditional approaches (Murthy and Mamo 2009*;* Singh *et al.* 2013*;* Talabi and Tijani 2011). Also, the results indicate that image data of the two satellite sensors are equally good for groundwater potential modelling (Figure 6).

Table 6: Summary of groundwater potential zones of both satellite data and their static water level

VES Number	Curve Type	Location	Static Water Level (m)	NigeriaSat-X	Landsat ETM+
1	KH	Lugbe	15.5	Very Low	Low
2	AKH	Gwagwa	12.0	Very High	Very High
3	H	Lugbe	16	Moderate	High
4	HA	Lugbe	16.5	Low	Very Low
5	HA	Wuse	10	High	High
6	H	Airport	16.5	High	Very High
7	HA	Wuse	9.5	High	Moderate
8	KH	Dakibu	10	Low	Moderate
10	AA	Gwarinpa	9.5	High	Very Low
11	KHA	Kuje Town	15.5	Very Low	Low
13	A	Apo	9	Moderate	Moderate
14	HAA	Garki	10	Moderate	Very High
15	HKH	Lugbe	12.5	Moderate	High
16	H	Lugbe	11	Very Low	Very Low
17	KH	Wuse	12	Low	Moderate
18	HKH	Dawaki	15.5	Low	Low
19	KHA	Dawaki	14.5	Very Low	Low
20	H	Wuse	10	Moderate	High
21	H	Jiru	16.5	High	Very High
22	HA	Airport Area	10	Very High	High
23	HAA	Kubwa Town	11	High	Very High
24	HA	Kuje Town	13.5	Very Low	Very Low
25	H	Area 1	12	Very Low	High
26	A	Zuba	23.5	Very Low	Very Low
27	HA	Idu	15	Low	Very Low
28	KH	Wuse	8.5	High	Very High
29	AKH	Garki	11	Low	High
30	H	Garki	11.5	Moderate	Low
31	HA	Jabi	14.4	Very Low	Low
32	HA	Wuse	10	Moderate	Low
33	H	Kubwa	11	High	High
34	HA	Maitama	10	High	Very High
35	KH	Asokoro	10	High	High

Analysis of the differences between NigeriaSat-X and Landsat ETM+ for groundwater potential modelling

Comparison of groundwater potential zones derived using NigeriaSat-X and Landsat ETM+ satellite data shows that there is a linear relationship between the two (Figure 6).

Thus, NigeriaSat-X satellite data can be used, together with other ancillary data, to generate groundwater potential zone variability of up to 96.72% of what Landsat ETM+ can do, and vice versa. Results of the paired-samples t-test show that at $\alpha = 0.5$, there was no significant difference in the performance of NigeriaSat-X (M=3.24, SD=0.67) and Landsat ETM+ (M=3.21, SD=0.94) satellite

data for groundwater potential modelling (t(62) = 0.17, p = 0.86).

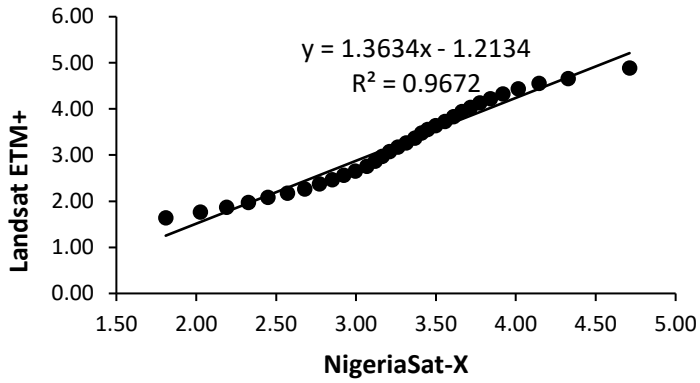

Figure 6: Correlation of groundwater potential of Landsat ETM+ and NigeriaSat-X satellite data

CONCLUSIONS AND RECOMMENDATIONS

This research compared the utility of NigeriaSat-X satellite data for groundwater potential modelling using the common and proven Landsat TM+ data as a base. Qualitative and quantitative evaluation of results derived from the two satellite data shows that significant similarities exist between them. The two imageries are very similar in quality and spectral bandwidth, though NigeriaSat-X has a better spatial resolution. The similarity of the band ranges and high-resolution images could make NigeriaSat-X a better substitute for Landsat ETM+ images for groundwater potential modelling.

The overall results demonstrate that there is no significance difference in the performance of NigeriaSat-X and Landsat ETM+ for groundwater modelling. However, the systematic data acquisition plan and well-established archival policy of the Landsat program which ensures global coverage and data availability, makes Landsat satellite data the choicest option over many other medium resolution data, including NigeriaSat-X. Further, the low cost of the imageries and free data distribution policy facilitate widespread access and applications. Keys to the wide use and popularity of Landsat imageries also include its large footprint and spatial/spectral resolutions fine enough to characterise terrain features. In all, the study found that the use of satellite imagery and GIS provide potentially powerful tools for the design of suitable exploration plan and water resources development in general. Further study is needed in the areas of band-to-band correlation between NigeriaSat-X and Landsat ETM+ and assessment of the potentialities in other areas of applications.

Acknowledgments

The authors thank the National Space Research and Development Agency (NASRDA) of Nigeria for making the NigeriaSat-X available, and the United States Geological Survey (USGS) for providing free access to Landsat ETM+ data.

REFERENCES

Aderoju OM, Patricia B, Oyewumi AS, Onuoha H (2014) Optimization of Nigerian Satellites in Flood Disaster Preparedness and Response IOSR Journal of Environmental Science, Toxicology and Food Technology 8:49-54

Agarwal E, Agarwal R, Garg RD, Garg PK (2013) Delineation of groundwater potential zone: *An AHP/ANP* approach J Earth Syst Sci 122:887-898 doi:10.1007/s12040-013-0309-8

Anomohanran O (2013) Geophysical Investigation of Groundwater Potential in Ukelegbe, *Nigeria* Joumal of Applied Sciences 13:119 - 125 doi:10.3923/jas.2013.119.125

Bhunia, GS (2020) An approach to demarcate groundwater recharge potential zone using geospatial technology. *Appl* Water Sci 10, 138 https://doi.org/10.1007/s13201-020-01231-1

Chatterjee, S, and S Dutta (2022) Assessment of groundwater potential zone for sustainable water resource management in south-western part of *Birbhum District, West Bengal. Appl Water Sci 12, 40(2022). https://doi.org/10.1007/s13201-021-01549-4*

Dar IA, Sankar K, Dar MA (2011) Deciphering groundwater potential zones in hard rock terrain using geospatial technology Environmental Monitoring and Assessment 173:597 – 610

Fashae OA, Tijani MN, Talabi AO, Adedeji OI (2014) Delineation of groundwater potential zones in the crystalline basement terrain of SW-Nigeria: an integrated GIS and remote sensing approach Applied Water Science 4:19 – 38

Ghosh A, Adhikary, PP, and B Bera (2022) Assessment of groundwater potential zone using MCDA and AHP techniques: case study from a tropical river basin of India. Appl Water Sci 12, 37 https://doi.org/10.1007/s13201-021-01548-5

Hussein AA Govindu V, Nigusse AGM (2017) Evaluation of groundwater potential using geospatial techniques Appl Water Sci 7

Ifediegwu, SI (2022) Assessment of groundwater potential zones using GIS and AHP techniques: a case study of the Lafia district, Nasarawa State, Nigeria. Appl Water Sci 12, 10. https://doi.org/10.1007/s13201-021-01556-5

Ikpaya OI, Onuh SO, Achem CU, Okehie BM, Madalla FY (2017) Pursuit of Nigeria into Space for Sustainable Development. In: Cruzen C, Schmidhuber M, Lee YH, Kim B (eds) Space Operations: Contributions from the Global Community. Springer International Publishing, pp 233-251. doi:10.1007/978-3-319-51941-8_11

Krishnamurthy J (2008) Comparative evaluation of Indian remote sensing satellite and landsat thematic mapper data for geological and geomorphological applications Geocarto International 6:39-52 doi:10.1080/10106049109354318

Malczewski J, Rinner C (2015) Multicriteria Decision Analysis in Geographic Information Science. Springer Science+Business Media, New York

Martin N, van de Giesen N (2005) Spatial Distribution of Groundwater Production and Development Potential in the Volta River basin of Ghana and Burkina Faso Water International 30:239 - 249

Meijerink AMJ (1996) Remote sensing applications to hydrology: groundwater Hydrological Sciences - Journal des Sciences Hydrologique 41:549 - 561

Meijerink AMJ, Bannert D, Batelaan O, Lubczynski MW, Pointet T (2007) Remote sensing applications to groundwater, Series on Groundwater No.16 edn. UNESCO, Paris

Murthy KSR (2000) Ground water potential in a semi-arid region of Andhra Pradesh - a geographical information system approach International Journal of Remote Sensing 21:1867 - 1884

Murthy KSR, Mamo AG (2009) Multi-criteria decision evaluation in groundwater zones identification in Moyale-Teltele subbasin, South Ethiopia International Journal of Remote Sensing 30:2729 – 2740

Nampak H, Pradhan B, Manap MA (2014) Application of GIS based data driven evidential belief function model to predict groundwater potential zonation Journal of Hydrology 513 283 – 300

Ogunmola JK, Ayolabi EA, Olobaniyi SB (2014) Lineament Extraction from SPOT 5 and NigeriaSat-X Imagery of the Upper Benue Trough, Nigeria Int Arch Photogramm Remote Sens Spatial Inf Sci XL-1:323-330 doi:10.5194/isprsarchives-XL-1-323-2014, 2014

Oguntoyinbo JS, Areola OO, Filani O (eds) (1978) A Geography of Nigerian Development. Heinemann Educational Books for the Regional Conference of the International Geographical Union, Nigeria,

Oikonomidis D, Dimogianni S, Kazakis N, Voudouris K (2015) A GIS/Remote Sensing-based methodology for groundwater potentiality assessment in Tirnavos area, Greece Journal of Hydrology 525:197–208

Ojigi ML (2005) Digital Terrain Modelling & drainage analysis of the Northern Part of Abuja Phase 11, Development Area, Using Geospatial Techniques.

Unpublished PhD Thesis, Fed. Univ. of Tech., Minna, Nigeria,

Okogbue CO, Omonona OV (2013) Groundwater potential of the Egbe-Mopa basement area, central Nigeria Hydrological Sciences Journal – Journal des Sciences Hydrologiques 58

Oladapo MI, Mohammed MZ, Adeoye OO, Adetola BA (2004) Geoelectrical Investigation of the Ondo State Housing Corporation Estate, Ijapo Akure, Southwestern Nigeria Journal of Mining and Geology 40:41 – 48

Osinowo, OO and KI Arowoogun (2020) A multi-criteria decision analysis for groundwater potential evaluation in parts of Ibadan, southwestern Nigeria. Appl Water Sci 10, 228. https://doi.org/10.1007/s13201-020-01311-2

Prasad RK, Mondal NC, Banerjee P, Nandakumar MV, Singh VS (2008) Deciphering potential groundwater zone in hard rock through the application of GIS Environ Geol 55:467 – 475

Rajesh, J, Pande, CB, and SA. Kadam (2021) Exploration of groundwater potential zones using analytical hierarchical process (AHP) approach in the Godavari river basin of Maharashtra in India. Appl Water Sci 11, 182 (2021). https://doi.org/10.1007/s13201-021-01518-x

Rao YS, Jugran D (2003) Delineation of groundwater potential zones and zones of groundwater quality suitable for domestic purposes using remote sensing and GIS Hydrological Sciences Journal 48:821 – 833.

Saaty TL (1980) The analytic hierarchy process: planning, priority setting, resource allocation. McGraw-Hill, New York

Saaty TL (1986) Axiomatic foundation of the analytic hierarchy process Management Science 32:841–855

Saaty TL (2004) Fundamentals of the analytic network process – multiple networks with benefits, costs, opportunities and risks J Systems Science and Systems Engineering 13:348-379

Saleh Y, Badr AM, F. EB, Shahata A (2014) Agricultural land-use change and disappearance of farmlands in Kaduna metropolis-Nigeria Science World Journal 9

Singh P, Thakur JK, Kumar S (2013) Delineating groundwater potential zones in a hard-rock terrain using geospatial tool Hydrological Sciences Journal 58:213 – 223

Srivastava PK, Bhattacharya AK (2006) Groundwater assessment through an integrated approach using remote sensing, GIS and resistivity techniques: a case study from a hard rock terrain International Journal of Remote Sensing 27:4599 – 4620

Talabi AO, Tijani MN (2011) Integrated remote sensing and GIS approach to groundwater potential assessment in the basement terrain of paper Ekiti area southwestern Nigeria RMZ – Materials and Geoenvironment 58:303 – 328

Wright EP (ed) (1992) The hydrogeology of crystalline basement aquifers in Africa vol 66. The Hydrogeology of Crystalline Basement Aquifers in Africa, Special Publications edn. The Geological Society, London. doi:10.1144/GSL.SP.1992.066.01.01